Protein-Based pH Sensor

DOI: 10.1002/anie.201204029

Converting a Solvatochromic Fluorophore into a Protein-Based pH Indicator for Extreme Acidity**

*Maiyun Yang, Yanqun Song, Meng Zhang, Shixian Lin, Ziyang Hao, Yuan Liang, Dianmu Zhang, and Peng R. Chen**

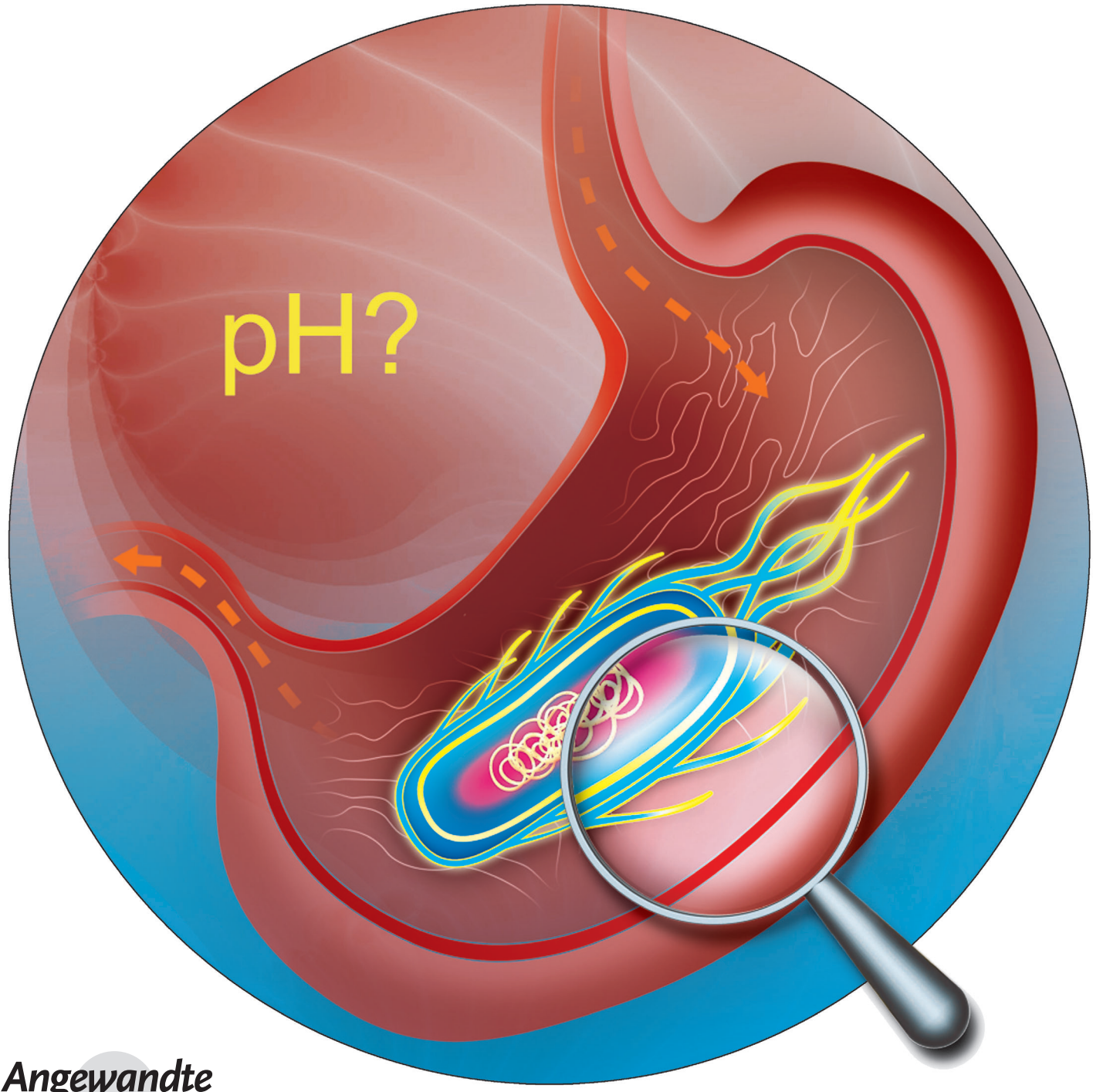

Maintaining pH homeostasis is fundamental for all living organisms.[1] The internal pH can vary from basic to highly acidic values in diverse prokaryotic species as well as in different subcellular compartments of eukaryotic cells.[1a,c,e,2] Although the extreme acidity (pH < 4) is fatal for the majority of living species, a large number of microorganisms including "acidophiles" and *Helicobacter pylori* have evolved to live under such harsh conditions.[1e,3] Another example is enteric pathogens, which are able to reach small intestine by passing through the highly acidic mammalian stomach, causing life-threatening infections. In eukaryotic cells, the acidic pH plays essential roles in many organelles, particularly those apparatuses along the secretory and endocytic pathways.[1a] However, despite of their fundamental roles, the precise pH values in these cellular compartments remain elusive, largely because of the lack of suitable probes for accessing the intracellular pH under highly acidic conditions.[1a,2]

Measuring the internal pH of living cells, particularly at a low pH value of less than 5, is challenging. The pH-sensitive green fluorescent proteins (GFPs) are widely used pH sensors for measuring the intracellular pH between pH 5 and pH 9.[4] However, these protein-based pH probes are not suitable for measuring more acidic pH levels since most proteins including GFPs will be denatured upon further acidification below pH 5. On the other hand, although many pH-sensitive fluorescent dyes have been used for imaging the acidic organelles by fluorescence microscopy,[5] they typically lack targeting specificity and the optimal working pH for each indicator relies on its own pK_a, which often results in a narrow working range. Certain acidic-organelle specific dyes have recently been developed, but they are usually weak bases with significantly perturbation on the pH in targeting organelles ("alkalizing effects").[6]

A key requirement for circumventing these challenges is to develop a genetically encoded pH probe that can sustain the extremely low pH conditions without "alkalizing effects". Inspired by a highly acid-stable and pH-responsive acid-chaperone HdeA in *E. coli*,[7] we aimed to develop a protein-based pH sensor for monitoring the extreme acidity by coupling the pH-mediated conformational change of HdeA with an environment-sensitive fluorescent dye. Such a fluorophore, termed solvatochromic fluorophore, has been shown to exhibit a low quantum yield in aqueous solution but becomes highly fluorescent in nonpolar solvents or upon binding to hydrophobic sites in proteins or membranes.[1a,8] As an essential acid-protection chaperone in *E. coli* periplasm, HdeA readily undergoes a pH-dependent conformational change and adopts a highly plastic structure when the pH value decreases from pH 7 to pH 2.[7] We reasoned that if such a conformational change can be converted to the fluorescent change of a solvatochromic fluorophore, it might be suitable for sensing the highly acidic pH in living samples. Furthermore, since the solvatochromic fluorophore itself is pH-insensitive and the assessment of pH will not depend on the pK_a value of a particular fluorescent dye, this strategy may result in an indicator capable of covering a broad pH range without "alkalizing effects". Herein we report the development of a protein-based, "solvatochromic" pH indicator for measuring the extremely low pH values in living cells.

To convert the pH-dependent conformational change of HdeA into a fluorescence signal change, we started by developing a general method for the site-specific attachment of an environment-sensitive fluorescent dye, 4-DMN (4-*N*,*N*-dimethylamino-1,8-naphthalimide),[1a] onto HdeA (Scheme 1). This fluorophore was chosen because it exhibits a higher sensitivity and a lower aqueous background than the commonly used environment-sensitive fluorophores such as PRODAN.[1a,8] We first verified that the fluorescence property of 4-DMN does not depend on pH changes (see Figure S1 a in the Supporting Information). In addition, the maximal emission wavelength of 4-DMN was found to shift from 550 nm in water to 505 nm in dioxane with a significantly increased fluorescence intensity (see Figure S1 b in the Supporting Information). To attach 4-DMN onto HdeA by a method compatible with living conditions, an alkyne-functionalized 4-DMN (alk-4-DMN) was first synthesized (Scheme 1 a). We next employed our recently developed azide-bearing unnatural amino acid (UAA)-ACPK (N^{ε}-

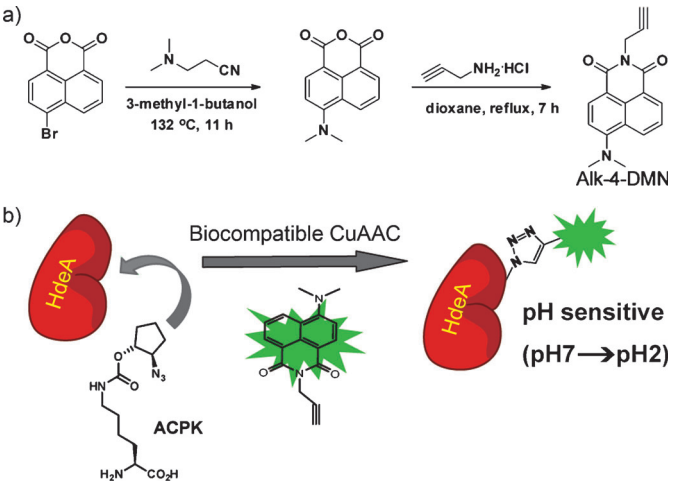

Scheme 1. Synthesis and labeling of an alkynal solvatochromic fluorophore onto the *E. coli* acid-chaperone HdeA. a) Synthesis of the alkyne-functionalized solvatochromic fluorophore 4-DMN (alk-4-DMN). b) A two-step "click-labeling" strategy for site-specific attachment of alk-4-DMN onto HdeA under living conditions.

[*] M.-Y. Yang,[+] Y.-Q. Song,[+] Dr. M. Zhang, S.-X. Lin, Z.-Y. Hao, Y. Liang, D.-M. Zhang, Prof. Dr. P. R. Chen
Beijing National Laboratory for Molecular Sciences
Synthetic and Functional Biomolecules Center
Department of Chemical Biology
Peking-Tsinghua Center for Life Sciences, Peking University
Beijing 100871 (China)
E-mail: pengchen@pku.edu.cn

[+] These authors contributed equally to this work.

[**] This work was supported by research grants from the National Key Basic Research Foundation of China (grant numbers 2010CB912300 and 2012CB917300), the National Natural Science Foundation of China (grant numbers 91013005 and 21001010), and Peking University.

Supporting information for this article is available on the WWW under http://dx.doi.org/10.1002/anie.201204029.

(((1*R*,2*R*)-2-azidocyclopentyloxy)carbonyl)-L-lysine) that can be genetically incorporated into the protein at an amber mutation site through an orthogonal pyrrolysyl-tRNA synthetase (PylRS)-tRNA pair.[9] Our previous characterization on the protein total mass and tandem mass spectrometry (MS/MS) confirmed that ACPK was able to be site-specifically incorporated into proteins without being reduced or modified inside *E. coli* cells.[10] This was further confirmed by MS/MS analysis on the ACPK-incorporated HdeA at residue 58 (HdeA58-ACPK, see Figure S2 in the Supporting Information). The HdeA protein carrying this site-specifically introduced azide handle can be subsequently conjugated with alk-4-DMN through biocompatible copper-catalyzed azide–alkyne cycloaddition (CuAAC, or termed "click" chemistry, Scheme 1 b).[9,11] Using this two-step protein "click-labeling" strategy, we were able to site-specifically append the 4-DMN fluorophore at any desired position on HdeA. This approach is particularly attractive since previous studies already demonstrated that the choice of the fluorophore as well as its attachment position and linker length are all essential for modulating the fluorescence responses of the generated sensory proteins.[8b,12] Therefore, although mutant aminoacyl-tRNA synthetase (aaRS)-tRNA pairs have been evolved to directly encode UAAs carrying certain fluorescent dyes such as coumarin and prodan,[13] this directed evolution approach is hardly feasible to conduct systematic optimization, which turns to be straightforward by using our two-step protein labeling strategy.

The acid-chaperone HdeA exhibits an amphiphilic feature with its N- and C-terminal regions heavily positive-charged and the internal region highly hydrophobic.[14] At neutral pH, HdeA forms a dimeric protein with one hydrophobic region constituting the dimer interface and the second hydrophobic region buried (Figure 1 a). Upon acidification, HdeA gradually exposes its two hydrophobic regions in a pH-dependent fashion from pH 7 to pH 2. When the pH value decreases to below 3, HdeA adopts a monomeric structure to bind to its substrates with a highly plastic conformation.[7] To identify the appropriate sites for attaching alk-4-DMN onto HdeA to generate the pH-dependent fluorescence signal, we chose a total of seven conjugation sites throughout HdeA sequence including the aforementioned hydrophilic and hydrophobic regions. An amber mutation (TAG) was created at each of these residues on HdeA followed by site-specific incorporation of ACPK (Figure 1 b, Supplementary Figure 3 a). These HdeA mutant proteins carrying a single-site incorporated ACPK at specific positions were conjugated with alk-4-DMN through biocompatible CuAAC, which exhibited similar labeling efficiency (Figure 1 c, Supplementary Figure 3 b,c). Further, the protein labeling efficiencies at four out of the seven HdeA-ACPK variants (residues: 7, 35, 58, and 72) were quantified by LC–MS[15] before and after alk-4-DMN conjugation, which all showed > 95 % conversion in vitro (see Figure S4–S7 in the Supporting Information).

Fluorescence spectra of each of these 4-DMN-conjugated HdeA variants were compared at pH 7 and pH 2, with the

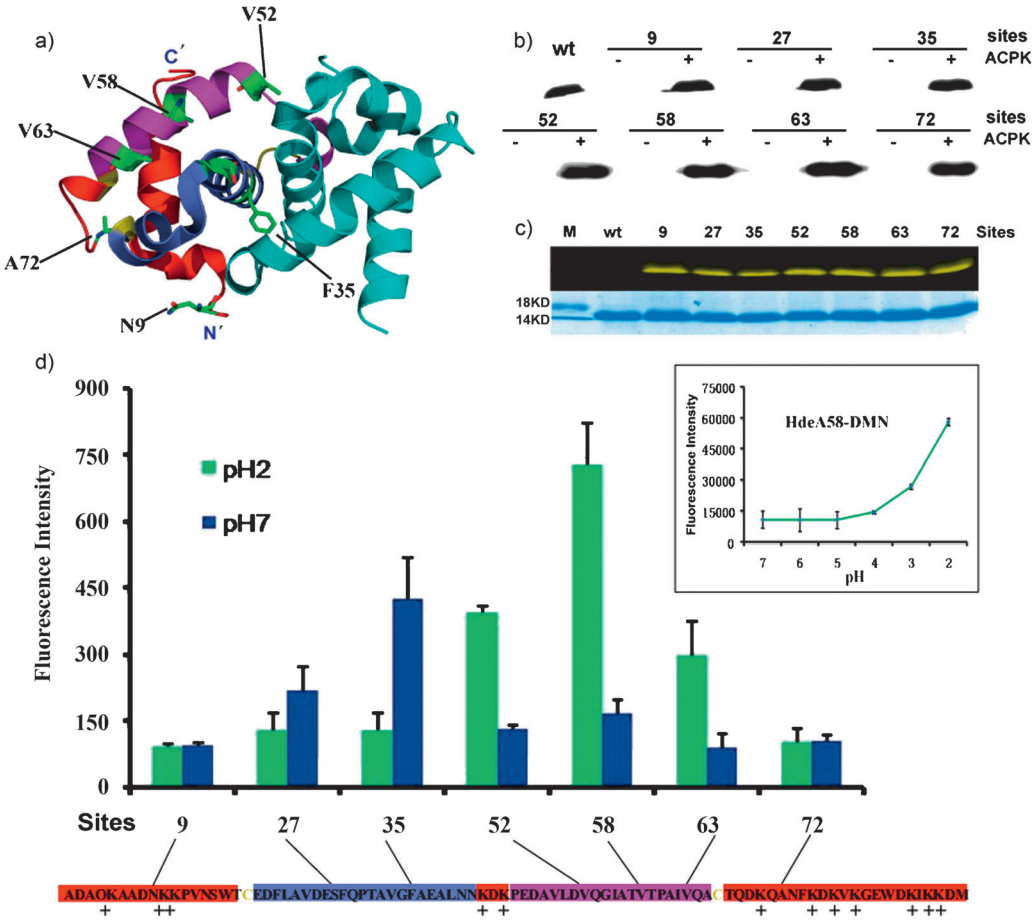

Figure 1. Systematic survey of the alk-4-DMN attachment site for an acid turn-on fluorescent sensor. a) The crystal structure of HdeA dimer protein with the ACPK incorporation site labeled. b) Immunoblotting analysis (anti-His) showing the incorporation of ACPK into HdeA-His_6 variants bearing a single amber mutation at each of the indicated site with (+) and without (−) 1 mM ACPK. c) SDS-PAGE analysis of the alk-4-DMN labeled HdeA protein variants visualized under UV illumination (top) or coomassie stain (bottom). d) Comparison of the fluorescence intensity of alk-4-DMN labeled HdeA variants between pH 7 (blue columns) and pH 2 (green columns). Inset: Fluorescence titration curve of the HdeA58-DMN probe as a function of the pH value (7.0–2.0).

excitation wavelength at 480 nm (Figure 1 d and Figure S8 in the Supporting Information). When 4-DMN was attached at residue Asn 9 or Ala 72 in hydrophilic terminus of the HdeA, we observed a low fluorescence intensity with negligible fluorescence changes at both pH 7 and pH 2. By contrast, a strong fluorescence appeared at pH 7 when 4-DMN was conjugated on residues (Ser 27 or Phe 35) at the hydrophobic dimer interface, whereas this fluorescence signal markedly decreased when the pH value dropped to pH 2. Interestingly, a significantly enhanced fluorescence signal was observed at pH 2 relative to pH 7 when 4-DMN was conjugated on residues (Val 52, Val 58, or Val 63) located in the second hydrophobic region. Since a fluorescent "turn-on" probe for the acidic pH is desired, we are highly interested in these HdeA variants with enhanced fluorescence upon acidification. Finally, to verify that the aforementioned fluorescent responses will not be perturbed upon binding to HdeA-substrates at pH 2, we compared the pH-dependent fluorescent changes of three representative HdeA variants (HdeA35-DMN, HdeA58-DMN, and HdeA72-DMN) with and without its model substrate (Figure S9 in the Supporting Information).[7c] The results indicated that unlike other variants such as HdeA35-DMN, the fluorescence change of HdeA58-DMN did not depend on its substrate.

The unique behavior of HdeA58-DMN prompted us to apply it for monitoring the pH conditions in living samples. We have recently shown that, by employing a biocompatible Cu^{I} ligand developed by Wu and co-workers,[11e] CuAAC was able to occur between the ACPK-incorporated protein and an alkyne-functionalized coumarin dye in the periplasmic space of *E. coli* cells without apparent toxicity.[9] To apply HdeA58-DMN in living cells, HdeA58-ACPK expressed in *E. coli* periplasm was first "click-labeled" with alk-4-DMN through the biocompatible CuAAC in the periplasmic space of living *E. coli* cells (see Figure S10 in the Supporting Information). The specificity of our CuAAC-mediated fluorescent labeling was confirmed by showing that no fluorescent labeled protein bands were detected when only alk-4-DMN but not the Cu^{I}/catalyst were present in cells. *E. coli* cells bearing the wild-type HdeA (HdeA-wt) protein were also used as a control, which did not yield any fluorescent protein bands upon treatment with alk-4-DMN and Cu^{I}/catalyst, further revealed that our live-cell fluorescent labeling was dependent on the ACPK amino acid, the alk-4-DMN fluorophore and Cu^{I}/catalyst, as well as on the PylRS-tRNA pair (Figure S11 in the Supporting Information). Next, the protein labeling efficiency was assessed by quantitative compassion of the fluorescence between equal amounts of HdeA58-ACPK proteins labeled by alk-4-DMN in *E. coli* cells at different time courses and the in vitro quantitatively labeled HdeA58-DMN (efficiency $> 95\,\%$), which showed about 80 % in vivo labeling efficiency within 90 minutes (Figure S10 in the Supporting Information). To further confirm that the protein labeling did not take place in bacterial lysate, a large excess of free 4-alk-DMN and Cu^{I} catalyst were added to the HdeA58-ACPK-expressing *E. coli* cells during the lysis process, which did not yield any fluorescence bands on PAGE gel (Figure S12 in the Supporting Information). Finally, to show that our pH-indicator can be used beyond bacterial periplasm, we constructed a cytosolic-expressed version of HdeA58-DMN by removing the periplasmic signaling peptide at the N-terminus of the HdeA. The BTTAA-assisted CuAAC-labeling (BTTAA = 2-[4-{(bis[(1-*tert*-butyl-1H-1,2,3-triazol-4-yl)methyl]amino)-methyl}-1H-1,2,3-triazol-1-yl] acetic acid) of the cytosolic HdeA58-ACPK protein by alk-4-DMN and its localization were verified (Figure S13 in the Supporting Information). Taken together, our experiments demonstrated the highly selective and efficient generation of HdeA-58-DMN through the two-step "click-labeling" strategy inside bacterial cells.

Next, we used fluorescence microscopy to directly visualize the fluorescence change of *E. coli* cells harboring HdeA58-DMN in its periplasmic space under various pH conditions (Figure 2 a). A faint fluorescence intensity was observed at pH 7 (Figure 2 a–i), whereas prompt increase in bacterial fluorescence was observed upon dropping the pH to 2.3 (Figure 2 a-iv), as determined by scanning confocal microscopy on live *E. coli* samples. Since the food-borne infectious diseases have been linked to the ingestion of *E. coli*-contaminated acidic foods,[2] we also incubated *E. coli* cells harboring HdeA58-DMN in apple cider (pH 3–3.5) or orange juice (pH 3.4) followed by visualization of these bacteria under a fluorescence microscope. Strong fluorescence signals were observed under both conditions (Figure S14), confirming that *E. coli* cells can live under such acidic environment that may serve as a source to cause infections. Further, to apply this strategy in mammalian cells, we displayed HdeA58-DMN on a mammalian cell surface followed by changing the pH in the surrounding environment. The gene encoding HdeA58TAG was inserted into the pDisplay vector (Invitrogen), which in conjunction with the pCMV plasmid expressing PylRS-tRNA pair allowed the presentation of the HdeA58-ACPK protein on the surface of BHK-21 cells (Figure S15). The subsequent conjugation with

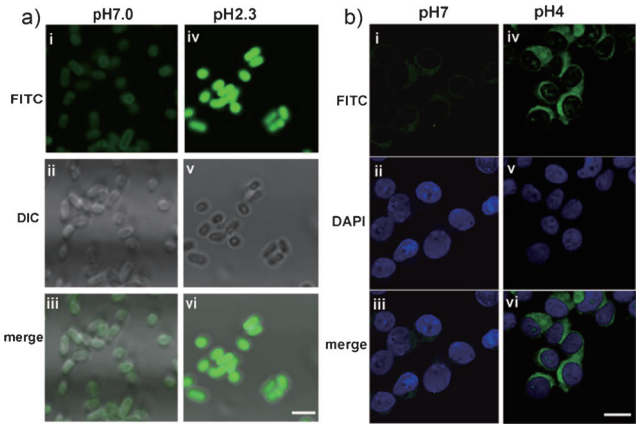

Figure 2. Visualization of the pH changes in *E. coli* and mammalian cells expressing HdeA58-DMN. a) *E. coli* cells expressing HdeA-58-DMN were visualized by a fluorescence confocal microscope in the fluorescein isothiocyanate (FITC) channel at pH 7 (i) and pH 2.3 (iv), respectively. Scale bar: 5 μm. b) BHK-21 cells expressing the surface-displayed HdeA-58-DMN were visualized by a fluorescence confocal microscope in the FITC channel at pH 7 (i) or pH4 (iv). Hoechst33342 was used to stain the cell nuclei (ii and v in the DAPI channel; DAPI = 4′,6-diamidino-2-phenylindole), while iii) and vi) are merged images from the FITC/DAPI channels. Scale bar: 10 μm.

alk-4-DMN through BTTAA-assisted CuAAC generated HdeA58-DMN on the BHK-21 cell membrane that can be visualized under a fluorescence microscope (Figure 2b-ii). A brighter fluorescence was observed upon lowering the extracellular space of BHK-21 cells from neutral to pH 4 (Figure 2b-iv). Applying HdeA58-DMN for monitoring pH changes in the acidic organelles along the endocytotic pathway of mammalian cells is currently underway in our laboratory.

To quantitatively measure the pH values in living cells, we coupled HdeA58-DMN with flow cytometry to determine the pH value in *E. coli* periplasm. This remains challenging because of the exceeding difficulty in specifically locating small molecule fluorophores in this space.[16] Because of the highly permeable outer membrane of *E. coli* cells, its periplasmic pH is equilibrated with the extracellular pH. To assess this periplasmic pH under highly acidic environment, we applied flow cytometric analysis on *E. coli* cells harboring the periplasmic-encoded HdeA58-DMN under a wide-range of pH values.

When the extracellular pH dropped from neutral to pH 2, an over fivefold fluorescence enhancement was observed from Flow Cytometer (Figure 3a). Neutralization of these acid-treated cells to pH 7 reduced the fluorescence signal to the initial level, indicating that HdeA58-DMN worked as a reversible pH sensor. The concentration of the sensory protein HdeA58-DMN was estimated to be 0.7×10^{-18} mol per *E. coli* cell (Supporting Information). No fluorescence changes were observed when flow cytometry was conducted on *E. coli* cells harboring the HdeA58-TAG gene in the absence of ACPK, alk-4-DMN, the CuAAC reagents or the PylRS-tRNA pair (Figure S16), confirming that the above fluorescence changes we observed were derived from the fluorescent labeled HdeA58-DMN. In addition, the C-terminal Histag was removed from the probe, which verified that Histag did not generate a "buffering effect" or interfere with the pH sensitivity of the indicator (Figure S17). Next, the pH values surrounding *E. coli* cells expressing HdeA58-DMN were reduced step-wisely from pH 7 to pH 2, which led to a gradually increased fluorescence signal at each step (Figure 3b). As an internal control, *E. coli* cells harboring HdeA72-DMN, a pH-insensitive fluorescent variant, gave a much smaller fluorescence change (smaller than twofold) upon acidification (Figure 3c). The fluorescence response curves of both HdeA58-DMN and HdeA72-DMN as a function of pH (7.0–2.0) were then recorded (Figure 3d). By calculating the relative fluorescence intensity (RFI) between these two variants at each pH point, a quantitative relation between relative fluorescence and pH values was obtained (Figure 3e). Finally, *E. coli* cells expressing the cytosolic expressed indicator (cyto-HdeA58-DMN) was also subjected to flow cytometric analysis at pH 7 and pH 2 (Figure S18). A smaller fluorescence increase was observed at pH 2 as opposed to *E. coli* cells harboring periplasmic-expressed HdeA58-DMN, indicating that the cytosolic pH value is higher than the periplasmic pH value under this highly acidic condition.

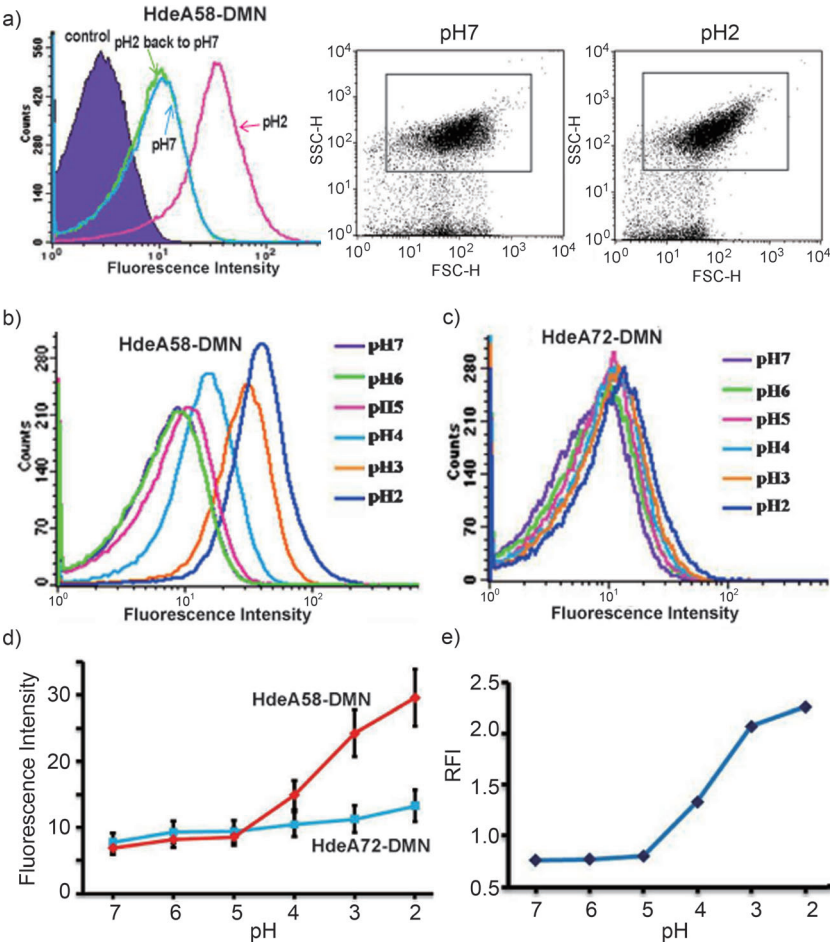

Figure 3. Monitoring the internal pH of living samples through flow cytometry. a) *E. coli* bacteria expressing HdeA58-ACPK were labeled with alk-4-DMN through biocompatible CuAAC followed by flow cytometric analysis at pH 7 (the cyan curve) and pH 2 (the magenta curve). *E. coli* cells harboring HdeA58-ACPK were used as the control. The corresponding dot plots of the flow cytometry histograms at pH 7 and pH 2 are shown on the right. b,c) Flow cytometry results of *E. coli* cells harboring variants HdeA58-DMN (b) or HdeA72-DMN (c) as a function of the pH value (7.0–2.0). d) The pH-dependent fluorescence response curves of HdeA58-DMN and HdeA72-DMN. Shown are the average results from three independently performed experiments. e) The relative fluorescence intensity (RFI) as a function of the pH value (7.0–2.0). The ratio of the fluorescence intensity between these two variants was calculated at each pH point to yield the RFI.

In summary, we have developed a protein-based, non-invasive pH indicator for monitoring a wide range of pH changes (pH 7 to 2) in living cells. Since a pH-insensitive solvatochromic fluorophore was employed in place of a commonly used pH-sensitive fluorescent dye, our probe features in a broad working range without "alkalizing effects". This

HdeA-derived pH indicator represents the first example, to our knowledge, that a protein-based pH sensor was used to noninvasively measure the extremely acidic extracellular pH that bacterial or mammalian cells might encounter under stressful conditions or during pathogenesis. Given its genetically encoded nature, our pH indicator may also become a useful tool for monitoring the intracellular pH in diverse prokaryotic and eukaryotic species. Finally, our strategy of using a site-specifically attached environmental-sensitive fluorophore to report the conformational change of a given protein may also be generally applicable for studying diverse protein-mediated cellular events.

Received: May 24, 2012
Revised: June 15, 2012
Published online: July 4, 2012

Keywords: click chemistry · fluorescence · pH indicators · proteins

[1] a) G. Loving, B. Imperiali, *J. Am. Chem. Soc.* **2008**, *130*, 13630 – 13638; b) G. Loving, B. Imperiali, *Bioconjugate Chem.* **2009**, *20*, 2133 – 2141; c) C. Baker-Austin, M. Dopson, *Trends Microbiol.* **2007**, *15*, 165 – 171; d) J. R. Casey, S. Grinstein, J. Orlowski, *Nat. Rev. Mol. Cell Biol.* **2010**, *11*, 50 – 61; e) T. A. Krulwich, G. Sachs, E. Padan, *Nat. Rev. Microbiol.* **2011**, *9*, 330 – 343.

[2] J. W. Foster, *Nat. Rev. Microbiol.* **2004**, *2*, 898 – 907.

[3] D. S. Merrell, A. Camilli, *Curr. Opin. Microbiol.* **2002**, *5*, 51 – 55.

[4] a) J. Llopis, J. M. McCaffery, A. Miyawaki, M. G. Farquhar, R. Y. Tsien, *Proc. Natl. Acad. Sci. USA* **1998**, *95*, 6803 – 6808; b) G. Miesenböck, D. A. De Angelis, J. E. Rothman, *Nature* **1998**, *394*, 192 – 195; c) M. C. Ashby, K. Ibaraki, J. M. Henley, *Trends Neurosci.* **2004**, *27*, 257 – 261; d) M. Kneen, J. Farinas, Y. Li, A. S. Verkman, *Biophys. J.* **1998**, *74*, 1591 – 1599.

[5] J. Han, K. Burgess, *Chem. Rev.* **2010**, *110*, 2709 – 2728.

[6] I. Johnson, M. T. Z. Spencer, *The Molecular Probes Handbook*, 11th ed., Life Technologies, California, **2010**.

[7] a) K. S. Gajiwala, S. K. Burley, *J. Mol. Biol.* **2000**, *295*, 605 – 612; b) W. Z. Hong, W. W. Jiao, J. C. Hu, J. R. Zhang, C. Liu, X. M. Fu, D. Shen, B. Xia, Z. Y. Chang, *J. Biol. Chem.* **2005**, *280*, 27029 – 27034; c) T. L. Tapley, T. M. Franzmann, S. Chakraborty, U. Jakob, J. C. A. Bardwell, *Proc. Natl. Acad. Sci. USA* **2010**, *107*, 1071 – 1076.

[8] a) M. E. Vázquez, J. B. Blanco, B. Imperiali, *J. Am. Chem. Soc.* **2005**, *127*, 1300 – 1306; b) G. S. Loving, M. Sainlos, B. Imperiali, *Trends Biotechnol.* **2010**, *28*, 73 – 83.

[9] Z. Hao, Y. Song, S. Lin, M. Yang, Y. Liang, J. Wang, P. R. Chen, *Chem. Commun.* **2011**, *47*, 4502 – 4504.

[10] S. Lin, Z. Zhang, H. Xu, L. Li, S. Chen, J. Li, Z. Hao, P. R. Chen, *J. Am. Chem. Soc.* **2011**, *133*, 20581 – 20587.

[11] a) Q. Wang, T. R. Chan, R. Hilgraf, V. V. Fokin, K. B. Sharpless, M. G. Finn, *J. Am. Chem. Soc.* **2003**, *125*, 3192 – 3193; b) M. G. Finn, V. Fokin, *Chem. Soc. Rev.* **2010**, *39*, 1231 – 1232; c) E. M. Sletten, C. R. Bertozzi, *Acc. Chem. Res.* **2011**, *44*, 666 – 676; d) Z. Hao, S. Hong, X. Chen, P. R. Chen, *Acc. Chem. Res.* **2011**, *44*, 742 – 751; e) D. Soriano Del Amo, W. Wang, H. Jiang, C. Besanceney, A. C. Yan, M. Levy, Y. Liu, F. L. Marlow, P. Wu, *J. Am. Chem. Soc.* **2010**, *132*, 16893 – 16899.

[12] M. Sainlos, W. S. Iskenderian, B. Imperiali, *J. Am. Chem. Soc.* **2009**, *131*, 6680 – 6682.

[13] a) H. S. Lee, J. Guo, E. A. Lemke, R. D. Dimla, P. G. Schultz, *J. Am. Chem. Soc.* **2009**, *131*, 12921 – 12923; b) C. C. Liu, P. G. Schultz, *Annu. Rev. Biochem.* **2010**, *79*, 413 – 444; c) J. Wang, J. Xie, P. G. Schultz, *J. Am. Chem. Soc.* **2006**, *128*, 8738 – 8739.

[14] Y. E. Wu, W. Hong, C. Liu, L. Zhang, Z. Chang, *Biochem. J.* **2008**, *412*, 389 – 397.

[15] C. D. Spicer, T. Triemer, B. G. Davis, *J. Am. Chem. Soc.* **2012**, *134*, 800 – 803.

[16] J. C. Wilks, J. L. Slonczewski, *J. Bacteriol.* **2007**, *189*, 5601 – 5607.

